Journal of the European Ceramic Society 20 (2000) 725–729

Reaction sintering of multicomponent mixtures for producing ceramics containing zirconia

T. Ebadzadeh*

Materials and Energy Research Center, PO Box 14155-4777, Tehran, Iran

Received 18 January 1999; received in revised form 15 April 1999; accepted 11 May 1999

Abstract

The effect of heat treatment on the phase evolution of the reaction sintering of zircon, clay, alumina and $Mg(OH)_2$ mixed powders were investigated. Final microstructures including porosities are correlated to the strength.

Keywords: Mechanical properties; Microstructure-final; Mullite; Reaction sintering; Spinel; ZrO_2

1. Introduction

The ternary system of ZrO_2–Al_2O_3–SiO_2 has brought complex system in which zircon, alumina, mullite, zirconia (tetragonal and monoclinic), pore and amorphous phases are simultaneously present during reactions. This intricacy becomes more unwell by introducing the cordierite phase. The dissociation phenomena in zircon finishes by prolonged heating (e.g. 6 h at 1675°C)[1,2] and forms ZrO_2 and amorphous SiO_2 which reacts with Al_2O_3 to yield mullite. Multicomponent toughened ceramic materials obtained by reaction sintering of $ZrSiO_4/Al_2O_3/MgO$ mixtures have been investigated.[3] These compositions are located in ZrO_2-mullite-spinel plane. The results showed that the dissociation temperature of zircon was reduced to <1425°C. As proved, mullite and cordierite containing ZrO_2 show higher strength and improved microstructure than mullite and cordierite without ZrO_2.[4,5] On the other hand, mullite-cordierite composites have low mechanical strength due to the low strength cordierite phase.[6,7] With increasing the cordierite content, the amount of pores and voids in mullite matrix increases which subsequently decreases the strength of the composite body.[6,8,9] It has been shown that 50/50 mullite-cordierite composite mixtures obtain the lowest strength due to the increasing of voids produced by sintering shrinkage and different thermal expansion between mullite and cordierite grains.[6]

In this study, the products of the reaction sintering of zircon, clay, alumina and $Mg(OH)_2$ mixtures were investigated by using XRD and SEM/EDX techniques. The effect of developed phases was studied on the strength and microstructure of composites.

2. Experimental procedure

The raw materials used were zircon (zircosil 5) supplied by Cookson Matthey Ceramics & Materials, α-alumina (CS-400 M) obtained from MARTOXID (Germany), English Clay (CC31) and $Mg(OH)_2$ (95 wt%) product of Merck. Table 1 shows the chemical composition of raw materials. The grain-size distribution of the zircon, clay and alumina powders were measured using a Fritsh particle size analysiett 22. The grain size varied from 0.25 to 3.57 μm for the zircon and from 0.76 to 11.65 μm for the clay. The particle size distribution of alumina powder was 90–95% lower than 1.6 μm. To obtain composite materials with mullite and cordierite (50/50) containing 10, 20 and 30 wt% zirconia (denoted as B10, B20 and B30, respectively) the composition of the mixed powders were selected. It would be expected that mullite, cordierite and zirconia with the above mentioned ratios would be obtained from the reaction sintering of mixed powders. The powders were milled in a planetary milling using alumina balls and containers with distilled water as milling medium for 1 h. The magnesium hydroxide particles were mixed with the clay particles in a wet state to prevent aggregation. Dilute HNO_3 was used for pH adjustment of the individual dispersed alumina and zircon powders before milling. The pH∼2 has been used in the present work. After

* Fax: +98-21-8773352.

0955-2219/00/$ - see front matter
PII: S0955-2219(99)00148-X

Table 1
The chemical composition of raw materials (wt%)

	Zircon	Clay	Alumina
SiO_2	37.3	47.8	$\leqslant$0.05
Al_2O_3	0.4	36.3	99.8
ZrO_2	59.5	–	–
TiO_2	0.12	0.1	0.005
MgO	0.03	0.2	0.2
CaO	0.04	0.1	0.01
Na_2O	0.22	0.1	$\leqslant$0.1
K_2O	0.01	2.8	–
Fe_2O_3	0.04	0.9	0.01
SO_3	0.16	–	–
P_2O_5	0.02	–	0.003
Loss on ignition	1	11.7	0.2

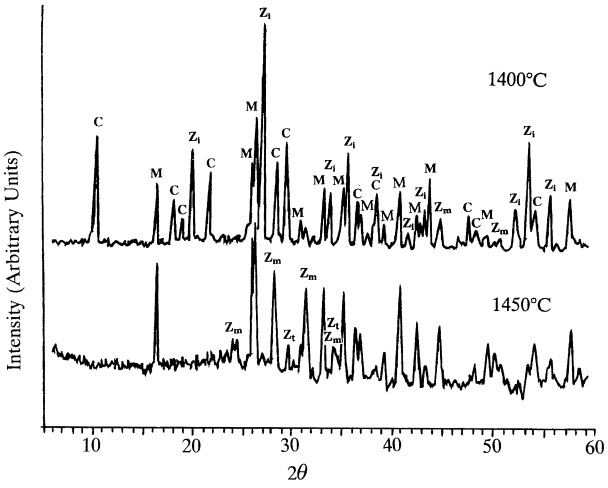

Fig. 1. Typical XRD patterns of B10 samples, held for 2 h at 1400 and 1450°C. C, α-cordierite; M, orthorhombic mullite; Z_i, zircon; Z_m, monoclinic zirconia; Z_t, tetragonal zirconia.

milling, the slurry was dried on the hot stage while being vigorously stirred. Oven dried cakes (at 110°C) were granulated through a 100 μm sieve. Mixed powders were uniaxially pressed at 170 MPa. The specimens were fired in an electric temperature controlled furnace (Carbolite RHF 17/10E) with the following heat regime :5°C/min to 150°C (30 min), 5°C/min to 600°C (60 min), 5°C/min to 900°C (60 min) and 10°C/min to 1450°C (120 min). The samples were allowed to cool from firing temperature in the furnace. The fired pellets were heat treated between 1200 and 1400°C (10°C/min) for 0.5, 1 and 2 h. X-ray diffraction was performed with a Philips X′ Pert system. The crystallinity of the samples was studied by comparing the relative intensities of the (110) α-cordierite, (111) monoclinic ZrO_2, (101) tetragonal ZrO_2, (111) cubic ZrO_2, (110) orthorhombic mullite, (113) α-alumina and (200) zircon peaks. The as-fired surface was used to preserve the concentrations of tetragonal and monoclinic zirconia. The bulk density of fired samples was measured by water displacement. Porosity measurements of heat treated samples were carried out according to ASTM-C373 (1969). Flexural strength measurements were made on bars (~36 by 6 by 5 mm) with a final surface polish of ~1 μm cut from heat treated pellets. Three-point bending tests were carried out in air and room temperature using an Instron testing machine with an outer span of 16 mm and a cross speed of 0.5 mm/min. At least eight bars were tested. Microstructural features were determined by scanning electron microscopy (Stereoscan 360, Leica Cambridge) on polished thermally etched samples (100°C below the sintering temperature for 30 min in air) and fracture surface of the bending test bars.

3. Results and discussion

Fig. 1 shows the typical XRD analysis results of the B10 composition sintered after 2 h at 1400 and 1450°C. The existence of the sharp zircon peaks after 2 h at 1400°C demonstrates incomplete reaction behaviour. By increasing the sintering temperature to 1450°C, mullite, monoclinic and tetragonal zirconia are the major crystalline phases while the traces of zircon peaks are found. Cordierite peaks are not observed which is common, due to the narrow firing range within 25°C of its incongruent melting point of 1455°C.[10] The B20 and B30 samples showed the same crystallisation behaviour as B10, just the sharper zircon peaks were observed at 1450°C. Development of cordierite phase in samples sintered at 1450°C was studied after 2 h at 1200, 1300 and 1400°C heat treatments (Fig. 2). As observed, the traces of cordierite peaks are distinguishable in samples treated after 2 h at 1200 and 1400°C. It means that the cordierite crystallisation from glass phase formed during sintering at 1450°C (cordierite melting) does not occur at 1200°C even after 2 h heat treatment. After 2 h heat treatment at 1300°C, the sharp cordierite peaks are elaborated, thus 1300°C was considered as the base temperature for development of the cordierite phase. As Figs. 2 and 3 show in all three combinations, the cordierite formation is accompanied with the zircon development. It seems that the formation of zircon at 1300°C is not just due to the recombination of ZrO_2 crystals with amorphous silica, because the relative intensity of ZrO_2 peaks is not considerably changed while the zircon peaks show the sharp increase of intensities in all three combinations (e.g. in the B20 composition the relative intensity of monoclinic zirconia reduced 18.5% while zircon increased 71% after extending the heat treatment from 1200 to 1300°C). It can be postulated that the formation of zircon at 1300°C is more due to the crystallisation of the glass phase formed from cordierite melting and zircon dissociation during the sintering of samples at 1450°C, as Pena and de Aza[2] confirmed the formation of transient-liquid phase as low as 1450 ± 10°C. The study of the

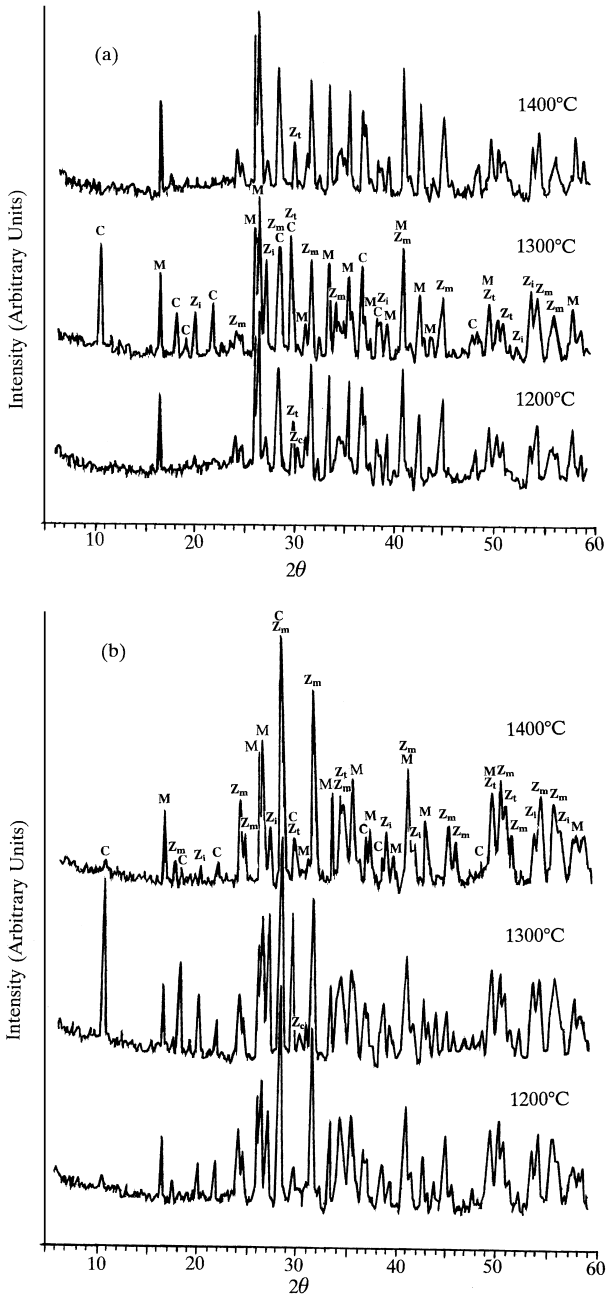

Fig. 2. Typical XRD patterns of sintered (a) B10 and (b) B30 samples after 2 h at 1450°C, heat treated at 1200, 1300 and 1400°C for 2 h holding time. C, α-cordierite; M, orthorhombic mullite; Z_i, zircon; Z_m, monoclinic zirconia; Z_t, tetragonal zirconia; Z_c, cubic zirconia.

contribution of tetragonal zirconia located in the neighbourhood of SiO_2 particles to the formation reaction of zircon at a lower temperature as Kanno[11] reported was not possible due to the interfering of tetragonal zirconia and orthorhombic cordierite main peaks. From the X-ray results, it can be determined that the complete removal of zircon is not possible due to the reactions between cordierite and ZrO_2 which becoming more intense at temperatures >1280°C.[4] By increasing the heating temperature to 1400°C (Fig. 2), again the

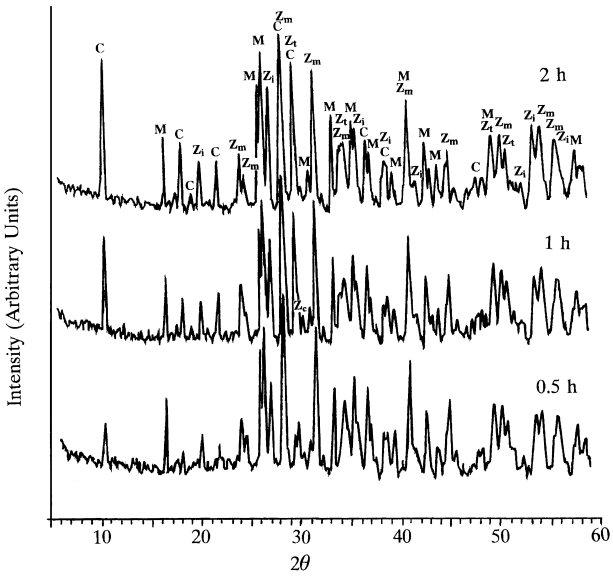

Fig. 3. Typical XRD patterns of sintered B20 samples after 2 h at 1450°C, heat treated at 1300°C for 0.5, 1 and 2 h holding times. C, α-cordierite; M, orthorhombic mullite; Z_i, zircon; Z_m, monoclinic zirconia; Z_t, tetragonal zirconia; Z_c, cubic zirconia.

dissociation of zircon and cordierite occurs simultaneously. Table 1 shows that used zircon and clay contain impurities which can promote the dissociation of zircon.[11] On the other hand, added $Mg(OH)_2$ to the powder mixtures for cordierite formation takes part in the dissociation of zircon by the formation of transient liquid.[3] As Fig. 2 shows, the intensity of the cordierite peaks is heightened by increasing the zircon component from B10 to B30 compositions, since the increasing of zirconia phase from the dissociation of added zircon promotes the cordierite crystallisation from the cordierite composition glass.[12,13] The study of the intensity changes of tetragonal zirconia was not possible because of the interfering of the tetragonal zirconia and orthorhombic cordierite peaks. The existence of tetragonal zirconia is proven by observing the individual (101) plane of tetragonal zirconia in heat treated samples at 1200°C (Fig. 2). The inhibition of the complete tetragonal to monoclinic phase trasformation at 1200°C could be ascribed to a blocking effect of silica which would hinder the growth of zirconia particles, keeping them below their critical size.[14] For studying the effect of heating time on the evolution of the cordierite, mullite and zirconia phases and the attenuation of zircon peaks, samples sintered at 1450°C were heat treated at 1300°C for different holding times. Fig. 3 shows the B20 samples, heat treated after 0.5, 1 and 2 h at 1300°C. As observed, the intensity of cordierite peaks increases by extending the heating times and alternatively the zircon peaks enlarge due to the recombination of ZrO_2 and amorphous silica. The results of the bending strength and porosity of heat treated samples are listed in Table 2. From these results and crystallisation behaviour of

heat treated samples at 1300°C (Figs. 2 and 3), it is found that the fracture strength is essentially dependent on porosity, cordierite and zirconia phases. Porosity formation can be attributed to two possibilities. First, vapour species evolved from the starting materials, such as OH and evaporating components from clay, or SO_2 from the zircon (Table 1). Second, the effect of cordierite and zirconia contents. As water evolution from cordierite glass and crystals is known to lead to large (5 μm) pores and bloating on high temperature sintering.[6] As Fig. 2 shows, increasing zirconia by the zircon component from B10 to B30 compositions, enhances cordierite phase and thus pores formation. On the other hand, B30 compositions, sintered at 1450°C and treated after 2 h at 1300°C [Fig. 2(b)], show the sharper cubic zirconia peak.

Increasing the porosity in B30 samples (Table 2) can be partially explained by the formation of the cubic phase which is responsible for the bloating (spherical voids) by releasing high pressure oxygen.[15] From Table 2, it is clear there is enhanced sintering by decreasing of pores from B10 to B20 compositions. Pores reduction accompanied with the strengthening grain boundary mechanism, produced by a continuous solid solution at the grain boundary between ZrO_2 and mullite, enhances grain boundary mass transport and consequently the sintering rate[16] and causes the increase of flexural strength. The strength decreasing from B20 to

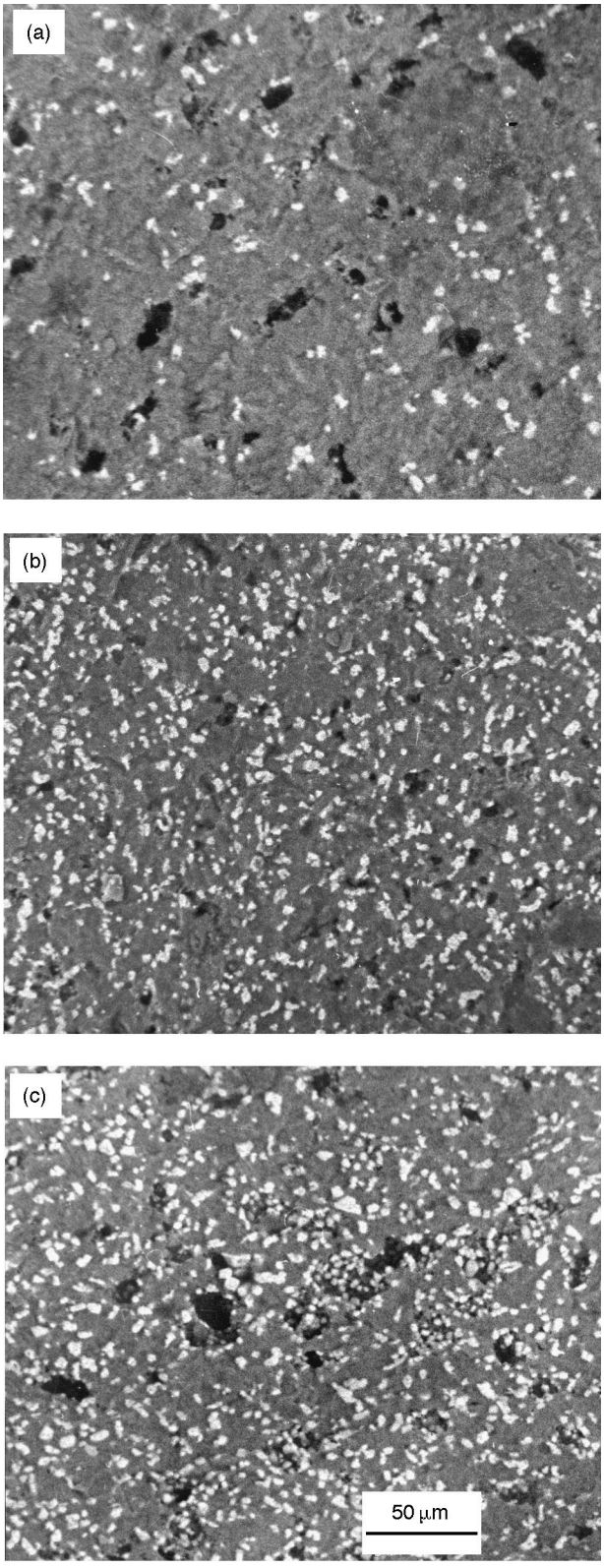

Fig. 4. Bend test fracture surfaces of samples sintered at 1450°C, heat treated for 2 h at 1300°C, (a) B10, (b) B20 and (c) B30.

Table 2
Porosity and flexural strength of composites sintered at 1450°C and heat treated after 2 h at 1300°C

Composition	Porosity (%)	σ_f (MPa)
B10	2.2 ± 0.1	155 ± 15
B20	1.5 ± 0.1	210 ± 18
B30	2.6 ± 0.2	158 ± 10

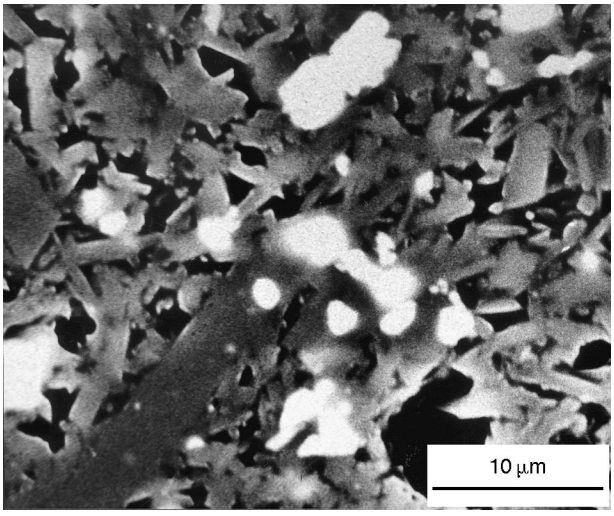

Fig. 5. SEM image of B10 sample sintered after 2 h at 1450°C, heat treated after 2 h at 1300°C (thermally etched 30 min at 1200°C) showing the more characteristic rod like structure of mullite.

B30 compositions (Table 2) can be attributed to four possibilities : (a) the intensified cordierite peaks (Fig. 2), then increasing pore content due to OH groups,[6] (b) the ZrO_2 particles, on cooling, relieve the strain by tetragonal to monoclinic transformation, resulting in extensive microcracking,[17,18] (c) the release of strain caused by the thermal expansion mismatch between mullite and cordierite,[6] and (d) the thermal expansion mismatch stresses between monoclinic ZrO_2 and cordierite resulting on cooling from temperatures below Tg gives rise to tensile microstress in the cordierite matrix.[4] Fig. 4 shows the backscattered electron images of fracture surfaces of the sintered composites at 1450°C heat treated at 1300°C for 2 h. As observed, all composites obtain homogeneous microstructures and as porosity measurements confirmed (Table 2), from B10 to B20 the pores diminished while from B20 to B30, again the increase of pores was distinguishable. Microstructural informations from SEM on both polished and fracture surfaces for the composites showed the rod like structure of mullite grains (Fig. 5).

4. Conclusions

Phase evolution results show that there are the boundary sintering conditions for cordierite phase development.

The sharp zircon peaks of the samples sintered at 1400°C indicate the incomplete reaction behaviour. Increasing the sintering temperature to 1450°C causes the dissociation of zircon associated with the removal of cordierite peaks.

The sharp α-cordierite peaks were observed in the samples sintered at 1450°C and heat treated after 2 h at 1300°C, while at 1200°C even after 2 h heat treatment the cordierite peaks were not observed. On the other hand, the cordierite peaks were not detected after 2 h heat treatment at 1400°C.

The B20 composites exhibit a positive effect on fracture strength at room temperature.

Acknowledgements

The author wishes to thank S. Noraei and F. Arkian for assistance with X-ray diffraction and electron microscopy, respectively.

References

1. Ansea, M. R., Biloque, J. P. and Fierens, P., Some studies on the thermal solid state stability of zircon. *J. Mater. Sci. Lett.*, 1976, **11**, 578–582.
2. Pena, P. and De Aza, S., The zircon thermal behaviour: effect of impurities, part 1. *J. Mater. Sci.*, 1984, **19**, 135–142.
3. Miranzo, P., Pena, P., Moya, J. S. and De Aza, S., Multicomponent toughened ceramic materials obtained by reaction sintering, part 2, system ZrO_2-Al_2O_3-SiO_2-MgO. *J. Mater. Sci.*, 1985, **20**, 2702–2710.
4. Travitzky, N. A. and Claussen, N., Microstructure and mechanical properties of cordierite-ZrO_2 composites. In *Advanced Ceramics II*, 1988, pp. 121–135
5. Kubota, Y. and Takagi, H., Preparation and mechanical properties of mullite-zirconia composites. In *Advances in Ceramics*, Vol. 24, 1988, pp. 999–1005.
6. Ebadzadeh, T. and Lee, W. E., Procesing-microstructure-property relations in mullite-cordierite composites. *J. Eur. Ceram. Soc.*, 1998, **18**, 837–848.
7. Anderson, R.M., Gerhardt, R. and Wachtman, J.B., Thermal, mechanical and dielectric properties of mullite-cordierite composites. In *Advances in Ceramics*, Vol. 26, 1989, pp. 265–277.
8. Mussler, B. H. and Shafer, M. W., Preparation and properties of mullite-cordierite composites. *Bull. Am. Ceram. Soc.*, 1989, **63**(5), 705–710.
9. Suzuki, H., Ota, K. and Saito, H., Preparation of cordierite ceramics from metal-alkoxides, part 2, sintering. *Yogyo-Kyokai-Shi*, 1987, **95**(2), 170–175.
10. Morrel, R., The mineralogy and properties of sintered cordierite glass-ceramics. *Proc. Brit. Ceram. Soc.*, 1979, **28**, 53–71.
11. Kanno, K., Thermodynamic and crystallographic discussion of the formation and dissociation of zircon. *J. Mater. Sci.*, 1989, **24**, 2415–2420.
12. Sue, Y. J., Chen, S. Y., Lu, H. Y. and Shen, P., Surface nucleation and cellular growth kinetics of cordierite glass ceramics containing 3 mol% Y_2O_3-ZrO_2. *J Mater. Sci.*, 1991, **26**, 1699–1704.
13. Watanabe, K. and Giess, E.A., Coalescence and crystallization in powdered high-cordierite ($2MgO.2Al_2O_3.5SiO_2$) glass. *J. Am. Ceram. Soc.*, 1985, **68**(4), C-102–C-103.
14. Nagarajan, V. S. and Rao, K. J., Crystallisation studies of ZrO_2-SiO_2 composite gels. *J. Mater. Sci.*, 1989, **24**, 2140–2146.
15. Lange, F. F., Shubert, H., Claussen, N. and Ruhle, M., Effects of attrition milling and post-sintering heat treatment on fabrication, microstructure and properties of transformation toughened ZrO_2. *J. Mater. Sci.*, 1986, **21**, 768–774.
16. Moya, J. S. and Osendi, M. I., Effect of ZrO_2 (ss) in mullite on the sintering and mechanical properties of mullite/ZrO_2 composites. *J. Mater. Sci. Lett.*, 1983, **2**, 599–601.
17. Ismail, M. G. M. U., Nakai, Z. and Somiya, S., Properties of zirconia-toughened mullite synthesized by the sol-gel method. In *Advances in Ceramics*, Vol. 24, *Science and Technology of Zirconia Ill, ACerS, OH*, 1988, pp. 119–125
18. Claussen, N. and Jahn, J., Mechanical properties of sintered, in situ-reacted mullite-zirconia composites. *J. Am. Ceram. Soc.*, 1980, **63**(3–4), 228–229.